AIP Advances

Piezoelectric properties of substitutionally doped β-Ga_2O_3

Cite as: AIP Advances **11**, 065111 (2021); https://doi.org/10.1063/5.0048975
Submitted: 28 February 2021 . Accepted: 20 May 2021 . Published Online: 03 June 2021

Lijie Li

Piezoelectric properties of substitutionally doped β-Ga_2O_3

Cite as: AIP Advances 11, 065111 (2021); doi: 10.1063/5.0048975
Submitted: 28 February 2021 • Accepted: 20 May 2021 •
Published Online: 3 June 2021

Lijie Li[a]

AFFILIATIONS

College of Engineering, Swansea University, Bay Campus, Swansea SA1 8EN, United Kingdom

[a]Author to whom correspondence should be addressed: L.Li@swansea.ac.uk

ABSTRACT

Modern semiconductor materials are increasingly used in multidisciplinary systems demonstrating cross-interactions between mechanical strains and electronic potentials, which gives rise to ubiquitous applications in high sensitivity, self-powered sensor devices. One of the fundamental prerequisites for such semiconductor materials to exhibit piezoelectric properties is the noncentrosymmetry of the crystal structures. β-Ga_2O_3 has been an emerging compound semiconductor material due to its ultra-wide bandgap. However, pristine β-Ga_2O_3 has an inversion center, displaying no piezoelectric effect. This work discovered that substitutionally doped β-Ga_2O_3 possesses piezoelectric property by using the first principles method, while a majority of previous research on its substitutional doping has been focused on the purposes of increasing electrical conductivity and formation of semiconductor heterojunctions. More interestingly, it is unveiled from this work that the formation energy has a clear relation with the piezoelectric coefficient.

I. INTRODUCTION

Gallium oxide (Ga_2O_3) has been increasingly investigated due to its ultra-wide bandgap (4.8 eV), which has sparked enormous research and development activities especially in areas of power electronics and solar blind UV photodetection.[1,2] Ga_2O_3 has five crystallographic phases—α, β, γ, δ, and ϵ. Among these phases, the β type is the most thermodynamically stable. It has a monoclinic crystal structure with Ga in the tetrahedral and octahedral sites.[3] On the contrary, a wide bandgap gives large resistivity, which hinders the material from being implemented in electronic devices. Moreover, special semiconductor types (i.e., *p*- and *n*-type) are often required in heterojunctions, which demands that β-Ga_2O_3 has to be intentionally doped. Here, in this work, it is focused on substitutional doping. Many research activities surrounding the β type have been doping of pristine β-Ga_2O_3 with various metals attempting to increase its conductivity so that it can be used to form diodes/transistors in practical applications.[4] Both *n*-type and *p*-type β-Ga_2O_3 have been achieved through substitutionally doping various metals such as using Sn doping to realize *n*-type[5] and using Zn doping to achieve *p*-type.[6] Strain induced polarization in modern semiconductor materials has attracted much attention due to its promising application in tunable devices with improved performance.[7,8] In order for the semiconductor materials to be piezoelectrically tunable, their crystal structures must display noncentrosymmetric property. Although β-Ga_2O_3 is superior in many applications, it does not exhibit piezoelectricity. So far, there have been very few reports on piezoelectricity of Ga_2O_3; there is one paper published recently reporting the piezoelectric property of ϵ-Ga_2O_3[9] based on first principles analysis, which is the only crystallographic phase that does not have an inversion symmetry among all Ga_2O_3 phases. Previously, the first principles method was widely used to study new material effects.[10,11] Here, for the first time, it is unveiled that substitutionally doped β-Ga_2O_3 possesses piezoelectric properties due to broken inversion symmetry caused by substitutionally doping with metal atoms. Detailed first principles analysis and discussions are described to elucidate this hypothesis.

II. ANALYSIS AND RESULTS

In the simulations, the monoclinic supercell of β-Ga_2O_3 has been built with 16 Ga atoms and 24 O atoms according to the crystal parameters in Ref. 12 (Fig. 1). The QuantumATK software has been used for simulation.[13] The supercell was then optimized using the generalized gradient approximations (GGA) and Perdew–Burke–Ernzerhof (PBE) exchange–correlation functional. The density mesh cutoff was set to 125 Hartree, and the k-point

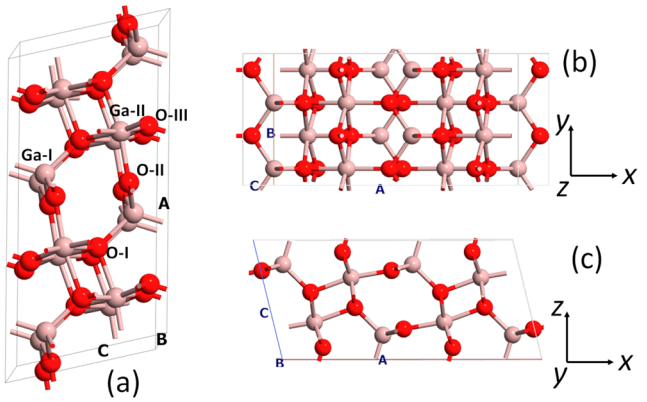

FIG. 1. (a) Crystal model of the β-Ga_2O_3 supercell containing 16 Ga atoms and 24 O atoms. (b) The 3D atomic structure showing different types of Ga and O locations. (c) The atomic structure in the *x*–*y* plane and the *x*–*z* plane.

sampling was 4 ×4× 4. In the geometry optimization setting, the force tolerance was 0.03 eV/Å, and the stress tolerance was set to 0.001 eV/Å^3. The optimized cell dimension is listed in Table I. The space group of the optimized β-Ga_2O_3 supercell is C2/m (group 12), which has an inversion center. The unit cell of β-Ga_2O_3 consists of two crystallographically different Ga atoms, one with tetrahedral (Ga-I) and the other with octahedral (Ga-II) coordination geometry. In addition, it contains three types of oxygen atoms (O–I, O–II, and O–III).[1] Before investigating the doped β-Ga_2O_3, analysis on the pure β-Ga_2O_3 was conducted to validate the simulation method by comparing the simulated band structure and density of state with previously reported ones. It has been well known that the GGA–PBE functional usually leads to underestimation of the bandgaps; therefore, a more accurate algorithm, Meta-GGA (MGGA), that takes local density $\rho(r)$ and the gradient of the density $\nabla\rho(r)$ into account, as well as the kinetic-energy density $\tau(r)$, is used. The difference between the GGA and MGGA is that the latter considers $\tau(r)$. Mathematically, the exchange potential $v_x^{TB}(r)$ is expressed as[13]

$$v_x^{TB}(r) = cv_x^{BR}(r) + \frac{3c-2}{\pi}\sqrt{\frac{4\tau(r)}{6\rho(r)}}, \quad (1)$$

where $\tau(r) = 1/2\sum_{i=1}^{N}|\nabla\psi_i(r)|^2$, $\psi_i(r)$ is the *i*th Kohn–Sham orbital and $v_x^{BR}(r)$ is the Becke–Roussel exchange potential. Parameter *c* can be extracted by fitting to the experimentally obtained bandgap. Here, in this work, parameter *c* was selected as 1.4, based on which the calculated bandgap for β-Ga_2O_3 is 4.8 eV. This bandgap is consistent with the value reported in experiments. The MGGA method has been used in calculating band structures and optical properties. MGGA is one of the generally adopted methods to correct the underestimated bandgap by the GGA,[14] which gives reasonable precisions as some other computationally expensive methods such as hybrid functionals (HSEs). Except for the bandgap value, the GGA is an appropriate method for calculating other properties. In this work, MGGA was used to calculate the bandgap and optical properties as the optical properties are mainly dependent on the band structures. The GGA was used to calculate the formation energies and piezoelectric coefficients, which has been considered as an appropriate approach.[15,16]

The electrical conductivity of intrinsic β-Ga_2O_3 is very low. As seen from Fig. 2(a), the valence band maximum is mainly formed by fully filled O 2p states, and the conduction bands in proximity to the fermi level are mainly occupied by the Ga 4s and 4p orbitals. To increase the electrical conductivity, β-Ga_2O_3 is usually doped by various metals, inducing additional donor or acceptor levels, corresponding to *n*- or *p*-type, respectively. Most notably, zinc (Zn) doping leads to increased acceptor levels (*p*-type conductivity),[6] and tin (Sn) doping causes increased *n*-type conductivity. It was reported that the resistivity of the Sn doped β-Ga_2O_3 film decreased from 1.79 ×10^7 to 0.12 **Ω**-cm as the Sn concentration increases from 0% to 10%.[17] Here, in this work, it is focused on metals that are located close to gallium on the Periodic Table, i.e., Ni (28), Cu (29), and Zn (30) on the same row as Ga (31), In (49), and Sn (50) on the next row, as these elements have a similar number of electrons in the outer orbitals. Only substitutional doping is considered in this work, which means the doping is implemented by replacing Ga atoms with one of the metals mentioned above. It was well reported that most metal atoms take the Ga-II position as the substitution position at Ga-II has a lower formation energy than that of Ga-I.[16] However, it is opposite for the Zn atom.[18] Hence, in the models, all types of metals take the position of Ga-II, except Zn. Precisely, the doped supercell is composed of 24 O atoms, 15 Ga atoms, and one other metal atom, corresponding to 6.25 at. % concentration. This doping concentration has been used in theory, which was compared with experiments.[19] In Ref. 20, 8 at. % Sn doped into Ga_2O_3 was used experimentally. MGGA simulation has been conducted for the substitutionally doped β-Ga_2O_3 for band structures and the projected density of states. From Figs. 2(b) and 2(c), it can be seen that Ni and Cu doping had a very similar impact on the bandgap, i.e., there are induced donor bands contributed by Ni 3d and Cu 3d orbitals, and the bandgaps remain similar to the undoped case, around 5 eV. This is understandable as Ni and Cu are adjacent to each other on the Periodic Table and have similar outer orbitals. With regard to Zn

TABLE I. Optimized lattice constants for β-Ga_2O_3 and its doped crystals.

	β-Ga_2O_3	Ni–Ga_2O_3	Cu–Ga_2O_3	Zn–Ga_2O_3	In–Ga_2O_3	Sn–Ga_2O_3
a	12.427 Å	12.384 Å	12.415 Å	12.496 Å	12.514 Å	12.553 Å
b	6.179 Å	6.171 Å	6.177 Å	6.189 Å	6.233 Å	6.247 Å
c	5.885 Å	5.881 Å	5.886 Å	5.868 Å	5.910 Å	5.942 Å
β	103.648°	103.589°	103.580°	103.472°	103.481°	103.614°

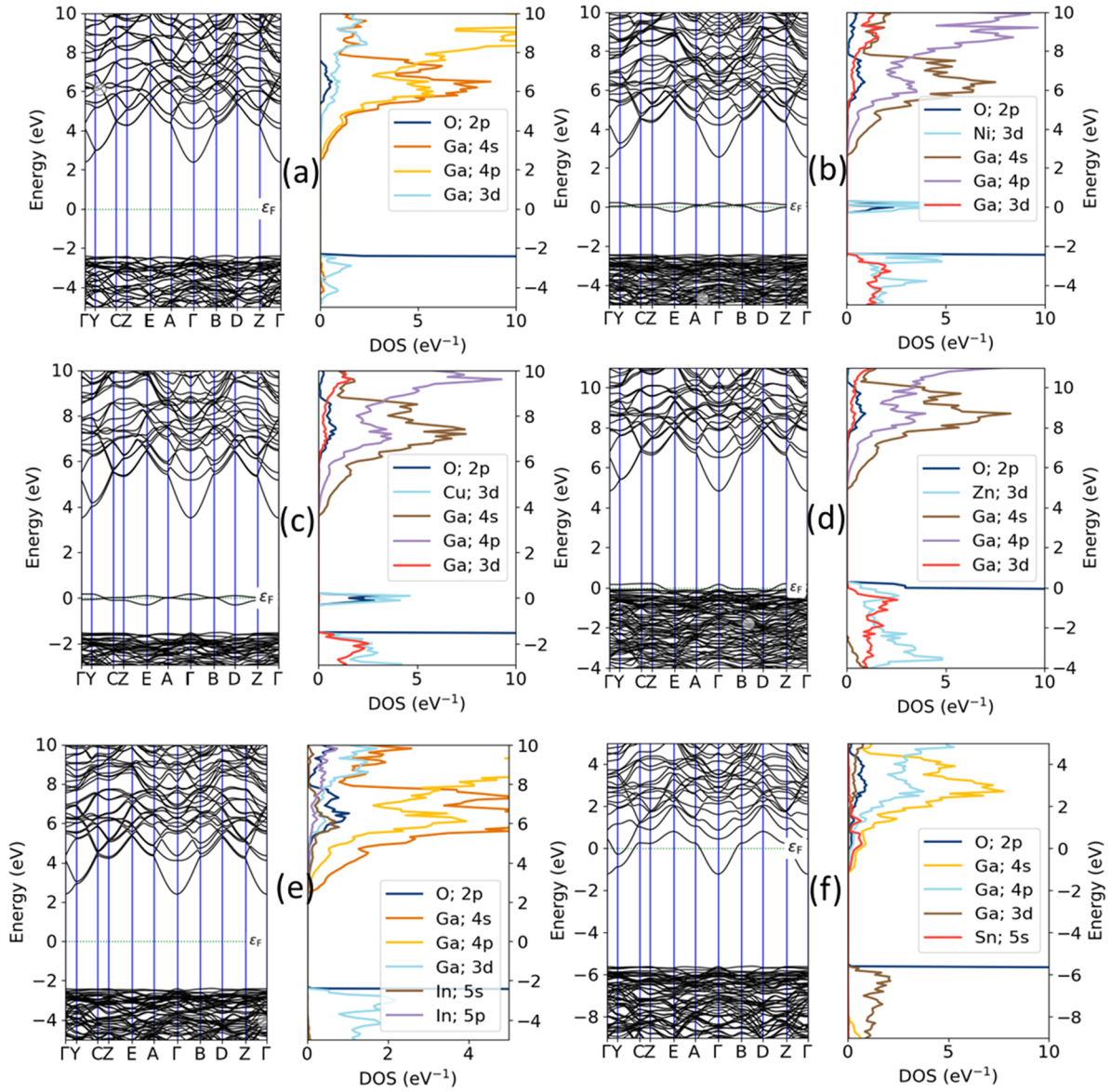

FIG. 2. Simulated band structures and electron density of states for various substitutionally doped β-Ga_2O_3 crystal structures: (a) intrinsic β-Ga_2O_3, (b) doped by Ni, (c) doped by Cu, (d) Zn doped, (e) In doped, and (f) Sn doped.

doping, the Zn atom takes the tetrahedral Ga position, inducing a shallow accepter energy level contributed by Zn 3d [Fig. 2(d)], which clearly displays *p*-type conductivity. This is consistent with previous experimental observation.[21] In doping has very little impact on band structures, i.e., the bandgap has been narrowed by around 0.1 eV [Fig. 2(e)]. Sn doped β-Ga_2O_3 has been very popular, and it induces *n*-type conductivity, which is attributed to the Sn 5s orbitals shown in Fig. 2(f).

Optical properties of pure β-Ga_2O_3 and doped β-Ga_2O_3 such as the absorption coefficient and refractive index can be derived from the density functional theory (DFT) calculations. The detailed procedure of these derivation processes was described in Refs. 22 and 23. In brief, the calculation started with the susceptibility tensor that determines the polarization level of the material due to an electric field. The complex dielectric constant was then deduced from the susceptibility tensor. The refractive index is related to the complex dielectric constant, and the optical absorption is related to the imaginary part of the dielectric constant.

The calculated refractive indices against wavelength for all doping configurations are very similar except for the Sn doped one that demonstrates significant differences from others. With regard to the absorption coefficient, the various doped β-Ga_2O_3 shown in

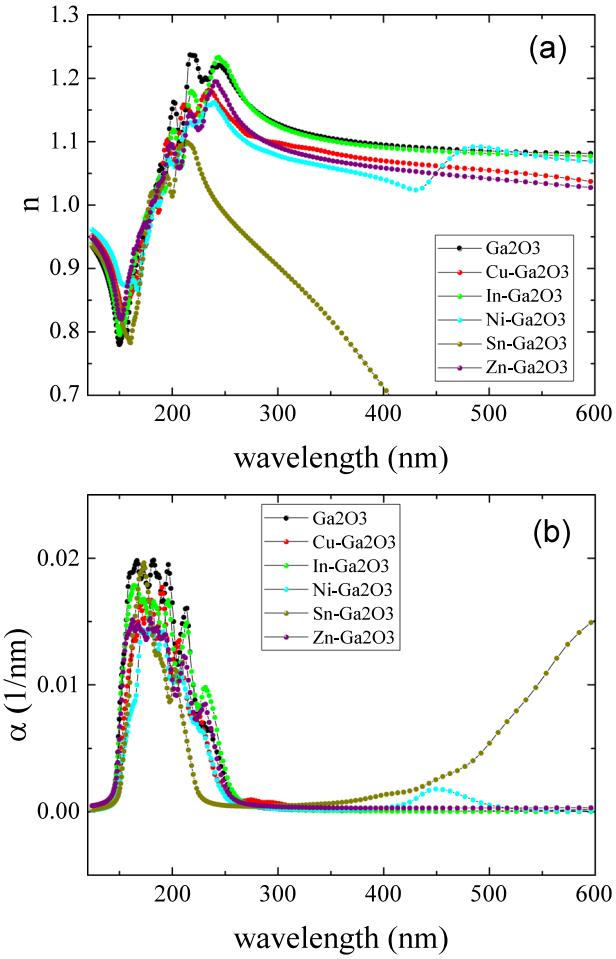

FIG. 3. Calculated optical properties of doped β-Ga_2O_3: (a) the calculated refractive index vs wavelength and (b) the calculated absorption coefficient vs wavelength.

Fig. 3(b) shows that the peak magnitudes of all cases under investigation at around 200 nm wavelength show a decreasing trend from pure to doped β-Ga_2O_3, especially for Zn and In doped cases. Nevertheless, all peak values in the band of 150–250 nm are between 0.015 and 0.02 nm^{-1}. This matches with the optical bandgaps for all these crystal structures. Interestingly, it shows a gradual increase in Sn doped β-Ga_2O_3 above 350 nm up to 600 nm wavelength.

Table I shows calculated optimized crystal dimensions for various doping conditions. The geometric optimization of substitutionally doped crystals followed the procedure described in Ref. 23. It is noted that the GGA in conjunction with the PBE functional has been used in the geometrical optimization procedure to relax the crystal structures in order to achieve minimum stress inside the crystal. As shown in Table I, slight variations appear for different doping configurations. For example, Cu and Ni doped β-Ga_2O_3 have slightly reduced dimensions, while Zn, In, and Sn doped β-Ga_2O_3 have increased crystal lattice parameters. Interestingly, as seen from the Periodic Table, Ni, Cu, and Zn have smaller atomic numbers than Ga. In and Sn have larger atomic numbers than Ga. Moreover, calculation has been conducted to arrive at the space group of the pristine β-Ga_2O_3 and doped cases. All cases investigated here are monoclinic crystals (Table II). It is found that the space group of pristine β-Ga_2O_3 is C2/m, which is centrosymmetric, displaying no strain induced polarization. This has been reported in the literature.[12] However, looking at the space groups of doped β-Ga_2O_3, they are all of Pm type, which does not have a center of symmetry. Clearly, this new finding leads to a plausible conclusion that substitutionally doped β-Ga_2O_3 will have piezoelectric properties, i.e., charges can be generated from mechanical strains. Further calculation has been conducted subsequently to obtain piezoelectric coefficients of doped β-Ga_2O_3.

Identical crystals structures are used as in the first part of Sec. II for piezoelectric coefficient calculation for pure β-Ga_2O_3 and doped cases in order to achieve consistent simulation results. It is focused on the piezoelectric coefficient in the "11" direction as only the *x*-axis aligns with direction *A*. The substitutionally Cu doped supercell in the *x*–*y* plane is shown in Fig. 4 (inset). The strain induced polarization is calculated using a Berry-phase approach using software, and e_{11} is calculated, which reflects the piezoelectric polarization along the x-axis (Fig. 4) subjected to strain in the x-axis. The calculated e_{11} for all crystal cases is summarized in Fig. 4. It is seen that Ni doped β-Ga_2O_3 has e_{11} of 4.74 C/m^2, and the e_{11} of Cu doped is 11.24 C/m^2. Zn doped β-Ga_2O_3 has e_{11} of 1.05 C/m^2. In and Sn doped β-Ga_2O_3 have values of 0.02 C/m^2 and 2.23 C/m^2, respectively. After showing the element position of the doping metals in the Periodic Table (see the inset in Fig. 4), one cannot help but link the piezoelectric coefficients of all cases with their atomic numbers. Ni and Cu are farther away to the left of the Ga atom, while Sn is farthest to the right of the Ga atom. These three doped crystals exhibit large piezoelectric coefficients. When the Ga atom is substituted by closer metal atoms in the Periodic Table such as Zn and In, the piezoelectric coefficient is much smaller.

Experimentally, detecting the exact location of diluted impurities in the β-Ga_2O_3 crystal lattice is challenging. One possibility is to measure the small changes in valence band density of states through x-ray photoelectron spectroscopy. Hence, one may comment that that the first principles simulation on the piezoelectric effect could be a speculation due to imperfectness or randomness of

TABLE II. Lattice type and space group for β-Ga_2O_3 and its doped crystals.

	β-Ga_2O_3	Ni–Ga_2O_3	Cu–Ga_2O_3	Zn–Ga_2O_3	In–Ga_2O_3	Sn–Ga_2O_3
Bravais lattice	Monoclinic	Monoclinic	Monoclinic	Monoclinic	Monoclinic	Monoclinic
Space group	C2/m	Pm	Pm	Pm	Pm	Pm
Piezoelectric	No	Yes	Yes	Yes	Yes	Yes

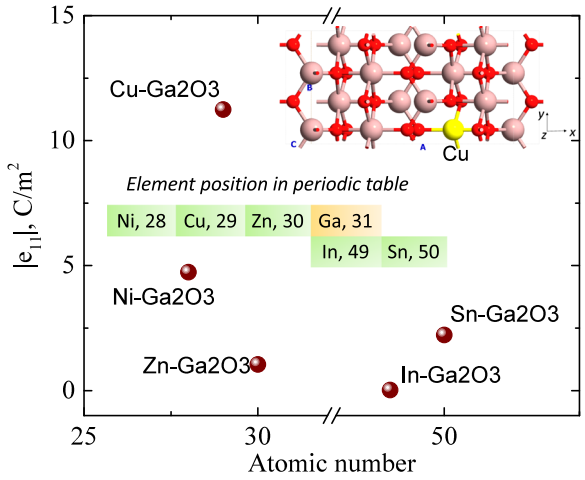

FIG. 4. Piezoelectric coefficient for doped β-Ga_2O_3. The inset graph shows doping elements in the Periodic Table. A simple Cu doped supercell is also shown at the top right corner of the figure.

substitutional doping in practical scenarios. More DFT simulations have been conducted with a larger size supercell using Sn doped β-Ga_2O_3 as an example containing 80 atoms ($Ga_{31}SnO_{48}$), which is twice diluted compared with the previous simulations. In addition, Sn has been placed randomly in two possible positions, as shown in Fig. 5(a) (Ga-II_1 and Ga-II_2) in this supercell. The two possible dopings are shown in Figs. 5(b) and 5(c). The values of e_{11} for these two doping cases are calculated to be 0.92 and 0.72 C/m^2, respectively. These values are approximately half of the value from the 40-atom model shown in Fig. 4. Taking imperfectness and randomness of doping in experiments into consideration, the calculation results show that substitutionally doped β-Ga_2O_3 will show piezoelectricity because e_{11} has the identical direction and will not cancel each other

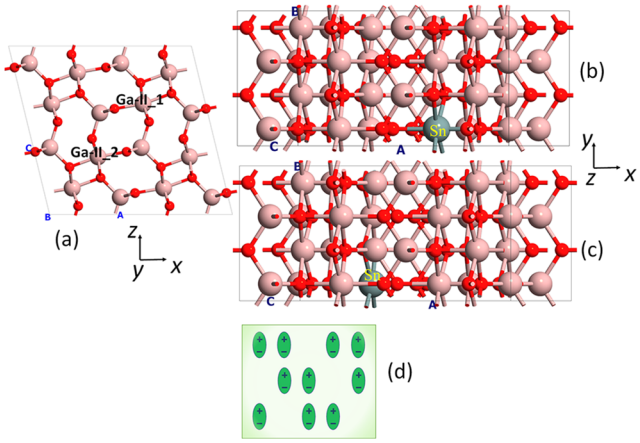

FIG. 5. Bigger model containing 80 atoms: (a) the model showing two possible Ga-II locations. (b) Sn doping in location 1 and (c) location 2. (d) A schematic illustration to show that the material will still demonstrate piezoelectricity despite imperfectness and randomness of the doping in experiments.

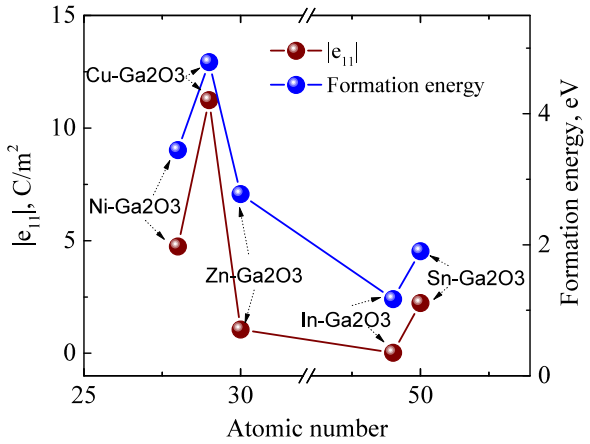

FIG. 6. Calculated formation energies in comparison with piezoelectric coefficients for various doping configurations.

[schematically depicted in Fig. 5(d)], but the actual experimental piezoelectric coefficient might be much smaller than the calculated values due to reduced impurity levels.

The formation energy (E_f) for a substitutionally doped β-Ga_2O_3 by various metals is defined as

$$E_f = E_{doped} - E_{bulk} + \mu_{Ga} - \mu_M, \quad (2)$$

where E_{doped} is the total energy of the metal doped β-Ga_2O_3, E_{bulk} is the total energy of the bulk material, and μ_{Ga} and μ_M are the chemical potentials of Ga and the dopant metal, respectively. Here, only the Ga-rich condition is considered, and the GGA was used to calculate the formation energies. Although GGA-predicted values are slightly smaller than those predicted by using the HSE method, it will have little effect in comparison with studies on various dopants.[16] Comparisons of calculated formation energies and piezoelectric coefficients for different doping conditions are shown in Fig. 6. It is seen from Fig. 6 that the formation energy is directly proportional to the piezoelectric coefficient. For instance, Cu doped β-Ga_2O_3has the largest formation energy as well as the largest piezoelectric coefficient. There is one exception where e_{11} of Zn doped β-$Ga_2O_3$is slightly lower than that of Sn doped β-Ga_2O_3. This is possibly due to the Zn atom taking the Ga-I position while all the other atoms take the Ga-II position. From optimized supercells for different doping configurations, the cell volume (CV) looks like another determining factor. The CVs of Ni, Cu, Zn, In, and Sn doped β-Ga_2O_3 are 436.9, 438.7, 441.3, 448.2, and 452.8 Å^3, respectively, while bulk Ga_2O_3 has a CV of 439.2 Å^3. On the same row as the Ga atom in the Periodic Table, the doping configurations with CVs closer to that of bulk Ga_2O_3 have larger piezoelectric coefficients. However, it is the opposite on the next row where In and Sn reside.

III. CONCLUSION

To summarize, density functional theory simulation has been conducted on doped β-Ga_2O_3. As opposed to undoped β-Ga_2O_3, substitutionally doped crystals do not have an inversion center, hence exhibiting piezoelectric performance. More study unveils that

the formation energy of the doped configurations is related to the magnitude of the piezoelectric coefficient. Larger formation energies of doped β-Ga_2O_3 will lead to stronger piezoelectricity. This investigation will hopefully serve as the tipping point in terms of applying doped β-Ga_2O_3 in the area of piezotronics.

ACKNOWLEDGMENTS

The author would like to thank the EPSRC Project (No. EP/T019085/1) and the European Regional Development Fund (ERDF) for funding the Solar Photovoltaic Academic Research Consortium (SPARC II).

DATA AVAILABILITY

The data that support the findings of this study are available from the corresponding author upon reasonable request.

REFERENCES

[1]J. Zhang, J. Shi, D.-C. Qi, L. Chen, and K. H. L. Zhang, "Recent progress on the electronic structure, defect, and doping properties of Ga_2O_3," APL Mater. **8**(2), 020906 (2020).
[2]D. H. Vieira, N. Badiei, J. E. Evans, N. Alves, J. Kettle, and L. Li, "Improvement of the deep UV Sensor performance of a β-Ga_2O_3 photodiode by coupling of two planar diodes," IEEE Trans. Electron Devices **67**(11), 4947–4952 (2020).
[3]L. Li, W. Wei, and M. Behrens, "Synthesis and characterization of α-, β-, and γ-Ga_2O_3 prepared from aqueous solutions by controlled precipitation," Solid State Sci. **14**(7), 971–981 (2012).
[4]M. Razeghi *et al.*, "A review of the growth, doping, and applications of β-Ga_2O_3 thin films," Proc. SPIE **10533**, 105330R (2018).
[5]D. Gogova, M. Schmidbauer, and A. Kwasniewski, "Homo- and heteroepitaxial growth of Sn-doped β-Ga_2O_3 layers by MOVPE," CrystEngComm **17**(35), 6744–6752 (2015).
[6]X. H. Wang, F. B. Zhang, K. Saito, T. Tanaka, M. Nishio, and Q. X. Guo, "Electrical properties and emission mechanisms of Zn-doped β-Ga_2O_3 films," J. Phys. Chem. Solids **75**(11), 1201–1204 (2014).
[7]W. Wu and Z. L. Wang, "Piezotronics and piezo-phototronics for adaptive electronics and optoelectronics," Nat. Rev. Mater. **1**(7), 16031 (2016).
[8]G. Michael *et al.*, "High-performance piezo-phototronic multijunction solar cells based on single-type two-dimensional materials," Nano Energy **76**, 105091 (2020).
[9]S.-D. Guo and H.-M. Du, "Piezoelectric properties of Ga_2O_3: A first-principle study," Eur. Phys. J. B **93**(1), 7 (2020).
[10]X. Ma, Y. Zhang, L. Dong, and R. Jia, "First-principles calculations of electronic and optical properties of aluminum-doped β-Ga_2O_3 with intrinsic defects," Results Phys. **7**, 1582–1589 (2017).
[11]K. A. Mengle and E. Kioupakis, "Vibrational and electron-phonon coupling properties of β-Ga_2O_3 from first-principles calculations: Impact on the mobility and breakdown field," AIP Adv. **9**(1), 015313 (2019).
[12]S. Geller, "Crystal structure of β-Ga_2O_3," J. Chem. Phys. **33**(3), 676–684 (1960).
[13]See www.synopsys.com/silicon/quantumatk.html for QuantumATK version Q-2019.12, Synopsys QuantumATK.
[14]F. Tran, J. Doumont, P. Blaha, M. A. L. Marques, S. Botti, and A. P. Bartók, "On the calculation of the bandgap of periodic solids with MGGA functionals using the total energy," J. Chem. Phys. **151**(16), 161102 (2019).
[15]F. Bernardini and V. Fiorentini, "First-principles calculation of the piezoelectric tensor d⇊ of III–V nitrides," Appl. Phys. Lett. **80**(22), 4145–4147 (2002).
[16]C. Tang *et al.*, "Electronic structure and optical property of metal-doped Ga_2O_3: A first principles study," RSC Adv. **6**(82), 78322–78334 (2016).
[17]X. Du *et al.*, "Preparation and characterization of Sn-doped β-Ga_2O_3 homoepitaxial films by MOCVD," J. Mater. Sci. **50**(8), 3252–3257 (2015).
[18]C. Zhang *et al.*, "Electronic transport properties in metal doped beta-Ga_2O_3: A first principles study," Physica B **562**, 124–130 (2019).
[19]Y. Zhang, J. Yan, G. Zhao, and W. Xie, "First-principles study on electronic structure and optical properties of Sn-doped β-Ga_2O_3," Physica B **405**(18), 3899–3903 (2010).
[20]S. Imura *et al.*, "Enhanced image sensing with avalanche multiplication in hybrid structure of crystalline selenium photoconversion layer and CMOSFETs," Sci. Rep. **10**(1), 21888 (2020).
[21]E. Chikoidze *et al.*, "p-type ultrawide-band-gap spinel $ZnGa_2O_4$: New perspectives for energy electronics," Cryst. Growth Des. **20**(4), 2535–2546 (2020).
[22]X. Cai, S. Deng, L. Li, and L. Hao, "A first-principles theoretical study of the electronic and optical properties of twisted bilayer GaN structures," J. Comput. Electron. **19**(3), 910–916 (2020).
[23]S. Deng, Y. Zhang, and L. Li, "Study on electronic and optical properties of the twisted and strained MoS_2/PtS_2 heterogeneous interface," Appl. Surf. Sci. **476**, 308–316 (2019).